Applied Catalysis B: Environmental 210 (2017) 454–461

Contents lists available at ScienceDirect

Applied Catalysis B: Environmental

journal homepage: www.elsevier.com/locate/apcatb

Ni-Co layered double hydroxides cocatalyst for sustainable oxygen photosynthesis

Mingwen Zhang[a], Zhishan Luo[a], Min Zhou[a], Guigang Zhang[a], Khalid A. Alamry[b], Layla A. Taib[b], Abdullah M. Asiri[b,c], Xinchen Wang[a,*]

[a] State Key Laboratory of Photocatalysis on Energy and Environment, College of Chemistry, Fuzhou University, Fuzhou 350002, PR China
[b] Chemistry Department, Faculty of Science, King Abdulaziz University, Jeddah 21589, Saudi Arabia
[c] Center of Excellence for Advanced Materials Research (CEAMR), Faculty of Science, King Abdulaziz University, Jeddah 21589, Saudi Arabia

ARTICLE INFO

Article history:
Received 25 February 2017
Received in revised form 27 March 2017
Accepted 31 March 2017
Available online 2 April 2017

Keywords:
Layered double hydroxides
Water oxidation cocatalysts
Carbon nitride nanosheets
Sustainable elements
Photocatalysis

ABSTRACT

The oxidation side of overall water splitting reaction, involving multiple electron transfer, O—H bond cleavage, and O—O bond formation, is a vital step to control the overall activities of water spitting. However, this process is usually restricted by the huge energy barrier and sluggish reaction kinetics. Recently, cobalt-based nanomaterials have been proved to be capable of decreasing the activation energy and accelerating the reaction kinetics. In principle, many factors will largely affect the activities, such as the loading contents, the size and structure of the cocatalysts. In order to achieve an overall enhancement of catalytic activities, it is reasonable to fabricate a tight and well matching junction that could efficiently promote the interface charge migration and separation. Herein, a high-performance water oxidation junction with layered structure was fabricated via *in-situ* growth of Ni-Co layered double hydroxides (LDHs) on graphitic carbon nitride nanosheets. Owing to the similarity of their layered stacking geometry, LDHs will strongly anchor on the surface of carbon nitride nanosheets, which could favor the photocatalytic water oxidation activities. As expected, the optimized binary catalysts showed remarkably enhanced activity for the photocatalytic water oxidation to release oxygen, which was 6.5 times higher than that of pure carbon nitride materials without loading the cocatalyst.

1. Introduction

H_2 production via photocatalytic water splitting over a semiconductor provides a promising technology for converting renewable and abundant solar energy to clean and storable chemical fuels in the form of chemical bonds [1–4]. However, the overall water splitting process is still restricted by the water oxidation half reaction, which involves four-electron transfer, O—H bond break and O—O bond formation, accompanying with high energy barrier of the reaction [5–8]. To overcome the sluggish water oxidation process, a widely used way is to deposit suitable co-catalysts on the surface of semiconductors to benefit the interface charge separation and as well as to accelerate the surface redox reaction kinetics [9–11]. Principally, the cocatalysts loaded on semiconductors could serve as an effective charge trap center to extract electrons or holes from the bulk to the surface, and thus suppress charge recombination to enable more separated electrons and holes for photocatalytic reactions. Thus, the coupling of suitable cocatalysts with photoenergy translator is a promising strategy to develop efficient photocatalytic systems for water splitting.

Recently, melon-based graphitic carbon nitride polymers with appropriate band structures for water splitting have been actively investigated as a promising semiconductor for visible light H_2 production from water [12–15]. However, the overall water splitting is very difficult to realize and usually hindered by the sluggish water oxidation process [16–18]. In order to promote the water oxidation activities, a series of cocatalysts have been well designed to decrease the energy barrier and facilitate the reaction kinetics at the soft surface [19–23]. For instance, a few amount of Co_3O_4 nanoparticles loaded on carbon nitride can greatly increase the rate of photocatalytic O_2 evolution from 2.8 $\mu mol \cdot h^{-1}$ to 25.1 $\mu mol \cdot h^{-1}$ under visible light irradiation ($\lambda > 420$ nm) [19] The Co_3O_4 nanoparticles not only could promote the water oxidation efficiency, but also enhance the O_2 evolution selectivity, which could largely restrain the self-oxidation process and reinforce the stability of the carbon nitride polymers. Besides, other cobalt-based materials, such as $Co(OH)_2$ [21] and $CoSe_2$ [23], have been also function as excellent cocatalysts to promote photocatalytic water

* Corresponding author.
E-mail address: xcwang@fzu.edu.cn (X. Wang).

http://dx.doi.org/10.1016/j.apcatb.2017.03.080
0926-3373/

oxidation activities. Very recently, a particular interesting is to develop a Co-based layered cocatalyst to better match the layer stacked graphitic carbon nitride, because the face-to-face contact between cocatalysts and carbon nitride nanosheets has a large interface region in view of the geometry.

Layered double hydroxides (LDHs) have shown excellent activities in photochemical water oxidation applications [24,25]. Compared with the single layered hydroxide, LDHs provide more possibilities to enrich their utilizations and further advancing the catalytic performance [26–28]. A typical example is that, few amounts of nickel incorporated with $Co(OH)_2$ could obviously enhance the stability for a long-time course reaction [25]. Besides, different transition metals always show different properties, which are contributed to expand their utilizations. In this paper, a series of Ni-Co LDHs were developed to serve as water oxidation cocatalyties to promote the photocatalytic O_2 evolution activities of carbon nitride. The molecular ratio of Co and Ni was controlled to examine the effect on the selectivity and activity of water oxidation for O_2 evolution. The as-prepared nanocomposites were then tested by solid characterizations to reveal the structure-performance relationship.

2. Experimental

2.1. Materials

Urea, $Ni(NO_3)_2.6H_2O$, $Co(NO_3)_2.6H_2O$, NH_4NO_3 and ammonia (30 wt.%) were purchased from China Sinopharm Chemical Reagent Co. Ltd. All reagents used in this work were of analytically pure grade and used as received without further purification.

2.2. Synthesis of photocatalysts

2.2.1. Synthesis of CNU

The carbon nitride nanosheets were prepared by a traditional thermal polymerization strategy with in-situ delamination. In typical route, urea (10 g) was placed in a crucible with a cover, and then it was annealed at 550 °C for 2 h with a ramping rate of 5.0 °C·min^{-1} in air. The final light yellow powder was then collected and donated as CNU.

2.2.2. Synthesis of nixCo3-x LDHs precursors

$Ni(NO_3)_26H_2O$, $Co(NO_3)_26H_2O$ ($[Ni^{2+} + Co^{2+}] = 1.0$ mmol), NH_4NO_3 (0.5 mmol) were dissolved in H_2O (3.5 mL) and 30 wt.% ammonia (1.5 mL) to form clear solution for further use. Four LDHs precursors were synthesized by changing the molar ratios of Ni^{2+} to Co^{2+} ($Ni^{2+}/Co^{2+} = 0$, 1, 1.5, 2) and named as Ni_0Co_3 LDHs, $NiCo_2$ LDHs, $Ni_{1.5}Co_{1.5}$ LDHs and Ni_2Co LDHs, respectively.

2.2.3. Synthesis of Ni_xCo_{3-x} LDHs/CNU

0.2 g of as-prepared CNU sample was immersed into 10 mL H_2O with ultrasonication for 10 min. Then, a certain amount of LDHs precursor, such as $NiCo_2$ LDHs, was dropwise added into the slurry above. The color of samples was changed from yellow to green immediately. The final resultant sample was washed by filtration with water and dried at 80 °C. The $NiCo_2$/CNU composites at 1 wt.%, 3 wt.% and 5 wt.% of LDHs loading were synthesized.

2.2.4. Synthesis of CoO_x/CNU

0.2 g CNU was impregnated into 4 mL water containing certain amount of $CoCl_2·6H_2O$ and the resulting solution were kept in ultrasonic bath for 1 min. After drying, the resulting mixture was calcined in air at 350 °C for 1 h.

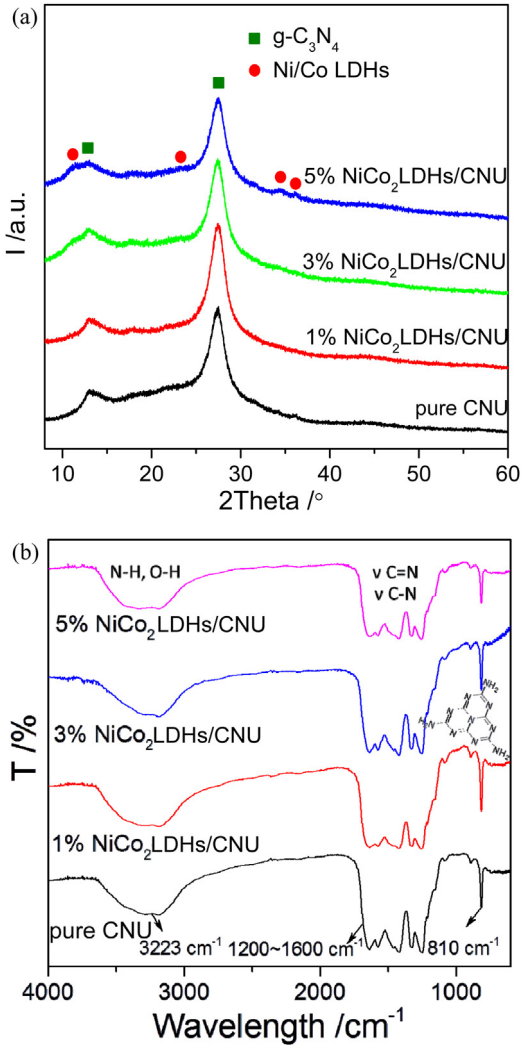

Fig. 1. (a) Power-XRD patterns and (b) FT-IR spectra of CNU and $NiCo_2$ LDHs/CNU samples.

2.2.5. Synthesis of Co_3O_4/CNU

The monodispersed Co_3O_4 nanoparticles were prepared using the previous method. [19] 0.2 g CNU was impregnated into 4 mL methanol containing certain amount of Co_3O_4 nanoparticles and the resulting solution were kept in ultrasonic bath for 1 min. After drying, the resulting mixture was calcined in air at 150 °C for 1 h.

2.3. Characterization

A Bruker D8 Advance diffractometer with Cu Kα1 radiation were employed to conduct X-ray diffraction (XRD) measurements. Fourier transformed infrared (FTIR) spectra were obtained on a Nicolet Magna 670 fourier transform infrared spectrometer. X-ray photoelectron spectroscopy (XPS) measurements were conducted on Thermo ESCALAB250 instrument with a monochromatized Al Ka line source (200 W). Transmission electron microscopy (TEM) was performed on a JEOL model JEM 2010 EX instrument. The UV–vis diffuse reflectance spectra (DRS) of the samples were conducted on a Varian Cary 500 Scan UV–vis spectrophotometer with barium sulfate as the reference. Photoluminescence (PL) spectra were collected on an Edinburgh FI/FSTCSPC 920 spectrophotometer. Electrochemical measurements were conducted with a BAS Epsilon Electrochemical System in a conventional three-electrode

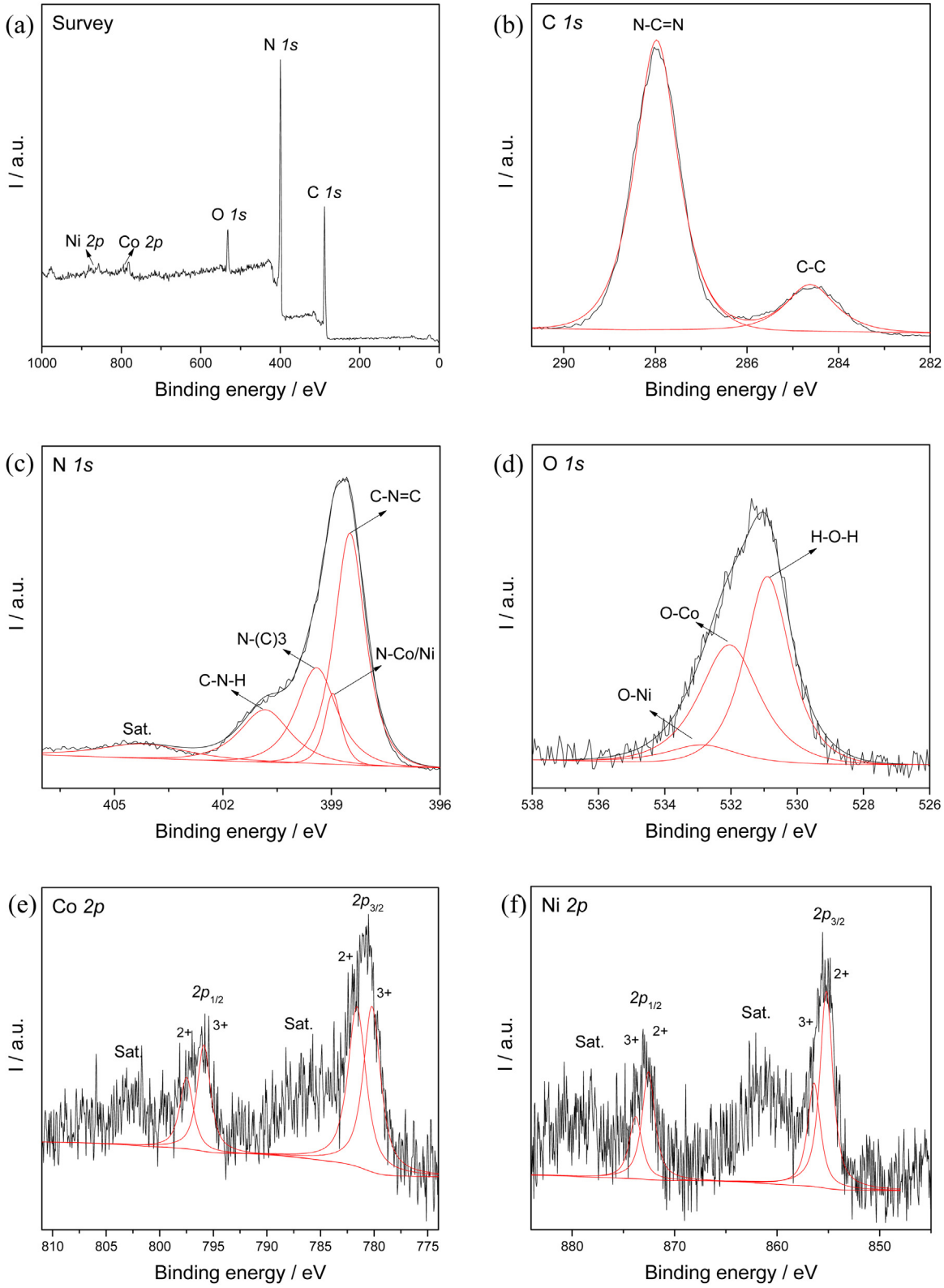

Fig. 2. XPS spectra of 3 wt.% $NiCo_2$ LDHs/CNU samples.

cell, using a Pt plate as the counter electrode and an Ag/AgCl electrode (3 M KCl) as the reference electrode. The working electrode was prepared on F-doped tin oxide (FTO) glass that was cleaned by sonication in ethanol for 30 min and dried at 353 K. The boundary of the FTO glass was protected using Scotch tape. A 5 mg sample was dispersed in 1 mL of DMF by sonication to give a slurry mixture. The slurry was spread onto pretreated FTO glass. After air drying, the working electrode was dried at 393 K for 2 h to improve adhesion. Then, the Scotch tape was removed, and the uncoated part of the electrode was isolated with epoxy resin. The electrolyte was 0.2 M Na_2SO_4 aqueous solution without additive (pH 6.8).

2.4. Photocatalytic test

Reactions were experimented with a Pyrex top irradiation reactor connected to a glass closed gas-circulation system. Water photooxidation was carried out by dispersing the catalyst (50 mg) in 100 mL aqueous solution containing different amount of metal compounds. After stirring for 30 min, silver nitrate (0.17 g, as the electron acceptor) and La_2O_3 (0.2 g, as the pH buffer agent) were added. The reactant solution was evacuated several times to remove air completely before irradiation under a 300 W xenon lamp with an appropriate cut-off filter. The temperature of the solution was maintained at 12 °C by a flow of cooling water during the reaction. The evolved gases were analyzed by a SHIMADZU GC-8A gas chromatograph with the thermal conductive detector, a 5 A molecular sieve column and using argon as the carrier gas.

3. Results and discussion

To examine the structure and phase information of the as-prepared $NiCo_2$ LDHs/CNU catalysts, Powder X-ray diffraction (XRD) technology was firstly carried out. It could be observed in Fig. 1a that CNU has two distinct diffraction peaks at 13.0° and 27.5°, corresponding to the repeating units (100) and the graphitic stacking (002) plane of typical graphitic carbon nitride, respectively [29–31]. As increasing the $NiCo_2$ LDHs from 1 wt.% to 5 wt.%, the peak intensity of (002) plane was gradually decreased, which could be mainly attributed to the strong interaction between metal cocatalysts and CNU. In addition, no noticeable change in crystal structure of CNU was observed, indicating the robust stability of the polymer to maintain the intrinsic properties. As a result of in-situ growth of Ni-Co LDHs on CNU, the Ni-Co LDHs were well-dispersed with significant aggregation, which was clearly demonstrated by the very weak diffraction peaks of Ni-Co LDHs.

The chemical structure of the $NiCo_2$ LDHs/CNU composites could also be confirmed by Fourier transformed infrared (FT-IR) spectroscopy. As shown in Fig. 1b, all samples show two feature-distinctive modes (810 cm^{-1} and 1200–1600 cm^{-1}), which are assigned to the triazine units breathing vibration and the aromatic C=N heterocycles stretching vibration, respectively, once again confirming the robust stability of the carbon nitride polymers [30]. The broad band at 3223 cm^{-1} was attributed to the stretching vibration mode of N—H or O—H. The N—H bond is mainly generated by the uncondensed terminal amino group, while O—H bond arises from the surface absorbed H_2O molecular from the air.

To further confirm the successful fabrication of layered double hydroxides on the polymer matrix, high resolution X-ray photoelectron spectroscopy (XPS) analysis was then conducted. As shown in Fig. 2a, the survey XPS spectra of the samples include C, N, O, Co, and Ni five species, first elucidating the existence of Co and Ni in the composite samples. In Fig. 2b and **c**, the high resolution C *1 s* and N *1 s* spectra of the as-prepared Co-Ni modified CNU samples are the same as that of the pure g-C_3N_4 polymers, once again certifying the successful evolution of CN heterocycle structure [30]. The O *1 s* spectra (Fig. 2d) could be deconvoluted into three peaks. The first peak centered at 530.9 eV is attributed to O—Ni bond while the second peak at 531.9 eV is assigned to O—Co bond, and they are usually associated with O in OH groups. The small third peak at 533.8 eV can be attributed to physic- and chemisorbed water [32]. Two distinct peaks at 781.0 eV (Co $2p_{3/2}$) and 796.4 eV (Co $2p_{1/2}$) with two small satellite (denoted as "Sat." in the figure) peaks are seen in the high-resolution Co *2p* spectrum (Fig. 2e). By using a Gaussian fitting method, the Co *2p* spectrum was best fitted with two spin-orbit doublets, which are in good agreement with the positions of both the Co^{2+} and Co^{3+} [33–35]. The similar two spin-orbit doubles characteristic of Ni^{2+} and Ni^{3+} and two shakeup satellites can been found in the Ni *2p* spectrum (Fig. 2f). These results show that the Ni-Co LDHs have a composition containing Co^{2+}, Co^{3+}, Ni^{2+} and Ni^{3+}. The metal cations are then available to incorporate with carbon nitride, which has a negative surface potential to generate the strong electronic coupling between metal cations and nitrogen-rich polymers. It is interesting to note that the binding energy of Co and Ni is lower in the value than that of the pure Ni-Co hydroxide previously reported [33]. This again suggests the strong chemical interaction between the Ni-Co LDHs and the surface electron-rich CNU polymers, forming strong layered junctions that are favorable for fast charge separation and collection at the polymer surface.

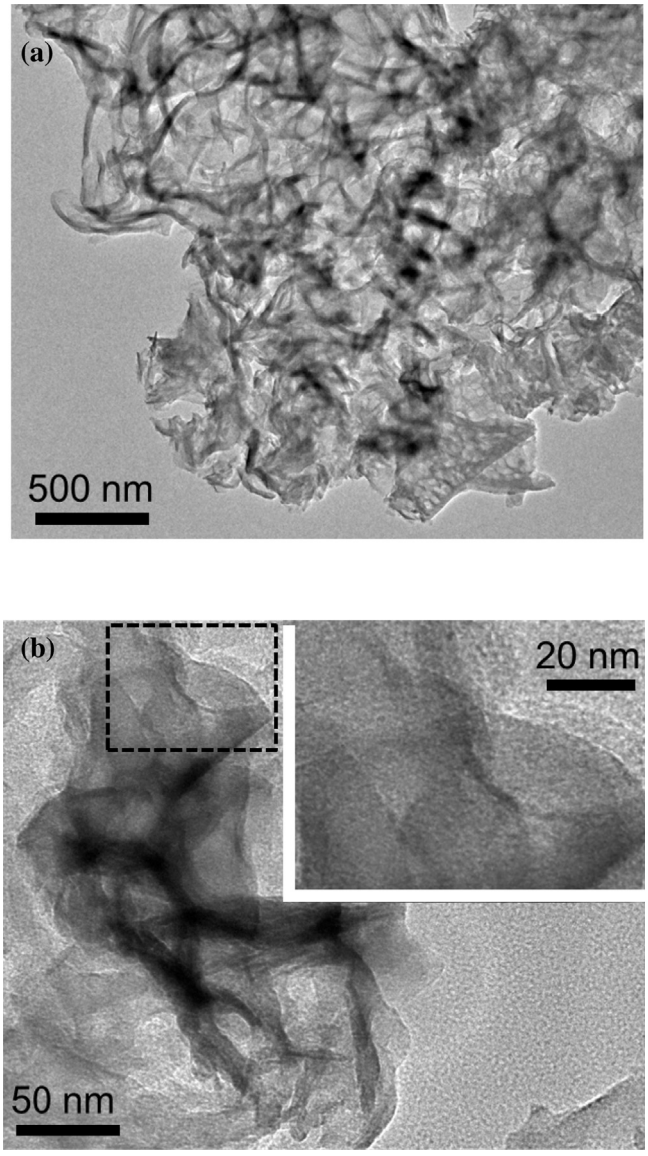

Fig. 3. (a) Typical TEM image of 3 wt.% $NiCo_2$ LDHs/CNU samples and (b) corresponding magnified image of the selected areas.

The morphology and texture structure of the resulting $NiCo_2$ LDHs/CNU sample were investigated by transmission electron microscopy (TEM). TEM images of CNU show typical curved platelet-like morphology with multi-hole structure, which are created by gas bubbles evolution (NH_3 and CO_2) during the pyrolysis process of urea (Fig. 3a) [36]. The structure of nanosheets with plenty of pores explains why a lot of amino groups were detected by FT-IR and XPS. Such coherent interface and lamellar morphology

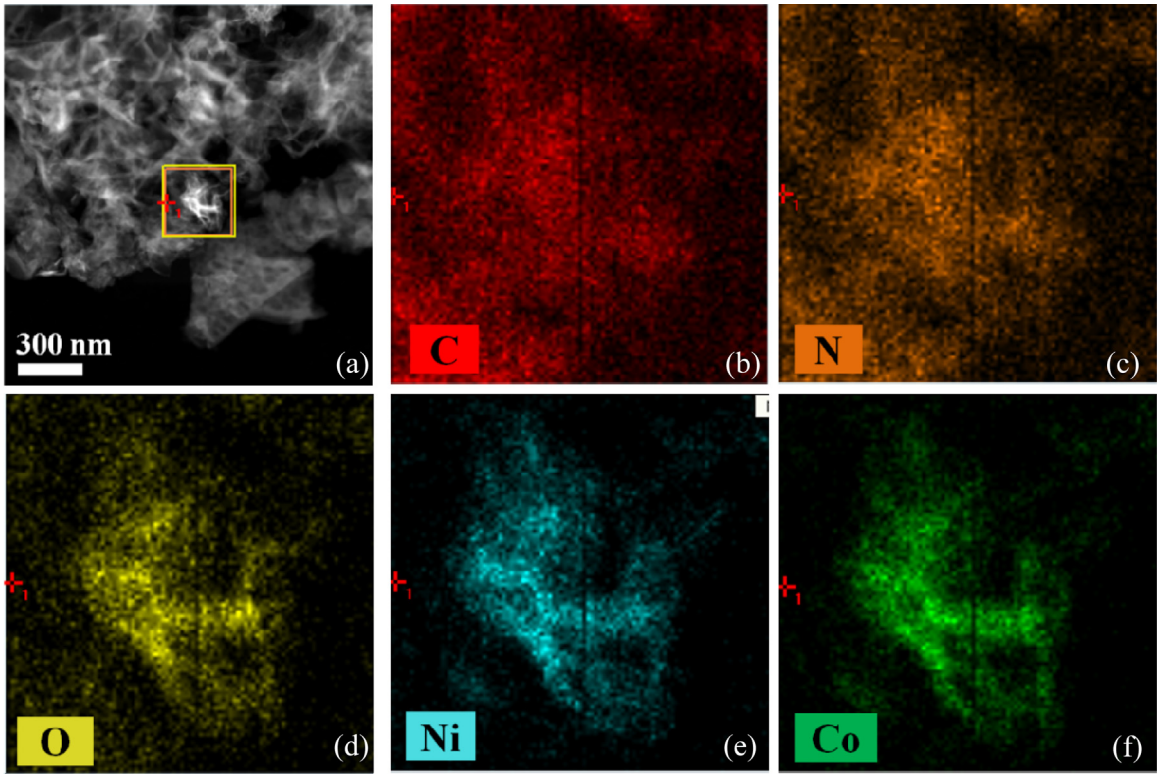

Fig. 4. (a) Scanning transmission electron microscopy (STEM) image; (b-f) elemental mapping images of C, N, O, Co and Ni for 3 wt.% $NiCo_2$ LDHs/CNU samples.

with rich N-containing docking sites is beneficial for LDHs to grow along the surface of CNU with strong interactions. As expected, the thin and silk-like LDHs intimately coated and stabilized by the CNU matrix without obvious aggregation. However, no lattice fringe could be observed in the magnified TEM image in Fig. 3b, further confirming the fabrication of amorphous Ni-Co LDHs at low temperature. Nevertheless, EDX elemental mapping (Fig. 4) clearly shows the well-defined spatial distribution of C, N, O, Co and Ni elements, indicating the homogeneous distribution of the Ni-Co LDHs on the surface of CNU, which is benefited for improving the surface redox reactions. The tight adhesion between the Ni-Co LDHs cocatalyst and CNU photocatalyst would greatly favor the interface charge carrier transfer and promote the photocatalytic activities.

Besides, the loading of Ni-Co LDHs on the surface of CNU would also generate positive effect on the optical/electronic properties. As shown in Fig. 5a, the UV–vis diffuse reflectance spectra (DRS) of the as-prepared samples exhibit the similar absorption band edge at about 440 nm, indicating that the deposition of cocatalyts would not change the band structure of the CNU polymers, which is accordance with the previous reports [30,31]. Note that an evident enhancement in the absorption could be observed in the region from 500 to 650 nm. The significant incensement in the optical absorption is attributed to the strong interaction between the transition metals and the oxygen[19], corresponding to the color change of sample from light yellow to grass green. However, this type of light absorption could not be utilized for excitation of CNU polymers to generation charge carriers. The charge carrier mobility could be examined by the room temperature photoluminescence (PL) spectra. As shown in Fig. 5b, a clearly decreased PL intensity could be viewed as the loading contents of cocatalysts increased from 1 wt.% to 5 wt.%. It is believed that the recombination of the charge carrier could be largely restrained. This is because the Ni-Co cocatalysts could act as charge carrier trap center to extract holes from the bulk of CNU to the interface of cocatalysts without recombination. The holes would then transfer to the surface of cocatalysts and subsequently participated in the surface redox reaction for O_2 evolution. Evidently, it will greatly improve the photocatalytic water oxidation activities.

To further confirm the positive role of $NiCo_2$ LDHs in promoting the water oxidation activities, electrochemical measurements were then performed in a typical three-electrode cell. Fig. 6a shows the current-potential curves of both pure and $NiCo_2$ LDHs loaded CNU electrodes. It could be seen that without the assistance of cocatalyst, pure CNU only presented rather low anodic current even the potential was as positive as 1.4 V (all potentials used are referenced to Ag/AgCl), indicating the huge energy barrier of the water oxidation process. However, when $NiCo_2$ LDHs was loaded on CNU sample, an abrupt onset of the catalytic anode current at 1.0 V was observed, which is ascribed from the fast oxidation of water to release O_2 gas. It is clearly to reveal that the $NiCo_2$ LDHs could indeed largely reduce the O_2 evolution overpotential, which is contributed to promote water oxidation activities. To further elucidate the generation and separation of photo-induced electron-hole pairs of the Ni-Co modified CNU polymers, the transient photocurrents of the samples were measured with positive bias voltage of 0.6 V. As shown in Fig. 6b, the transient photocurrent density of 3 wt.% $NiCo_2$ LDHs/CNU is much higher than that of the pure CNU. This enhancement in the photocurrent is probably resulted from the distinct reduced over-potential and efficient charge separation and transfer of photo-generated electron-hole pairs within the intense nanojunction between transition metals and CNU polymers.

Based on the above discussions, it is believed that the Ni-Co LDHs cocatalysts would act as excellent kinetics promotes to improve the oxygen-evolution reaction of the CNU polymers. The photocatalytic water oxidation performance of the as-prepared LDHs/CNU samples was then evaluated in an assay of O_2 evolution in the presence of electron acceptors (silver nitrate, 0.1 M). The experimental details could be seen in the experimental sec-

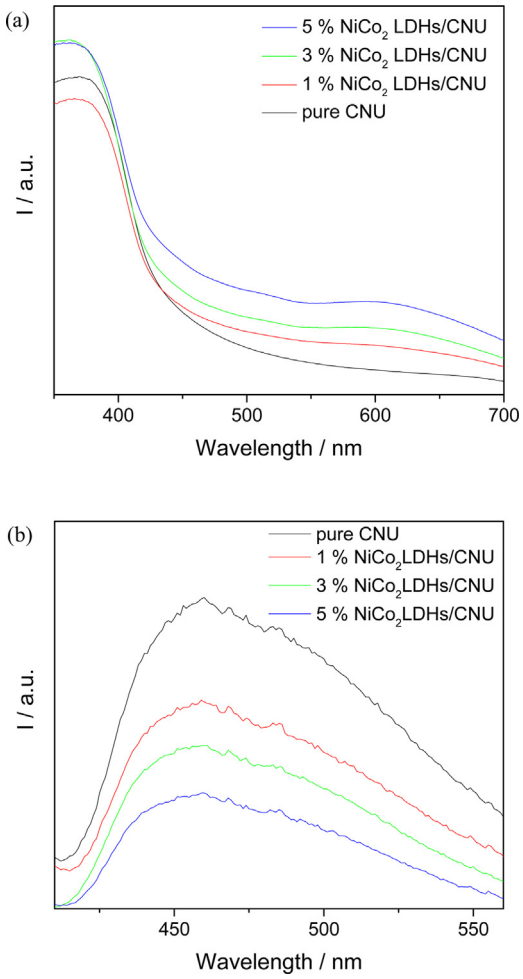

Fig. 5. (a) UV–vis DRS spectra and (b) room-temperature PL spectra under 400 nm excitation of CNU and $NiCo_2$ LDHs/CNU samples.

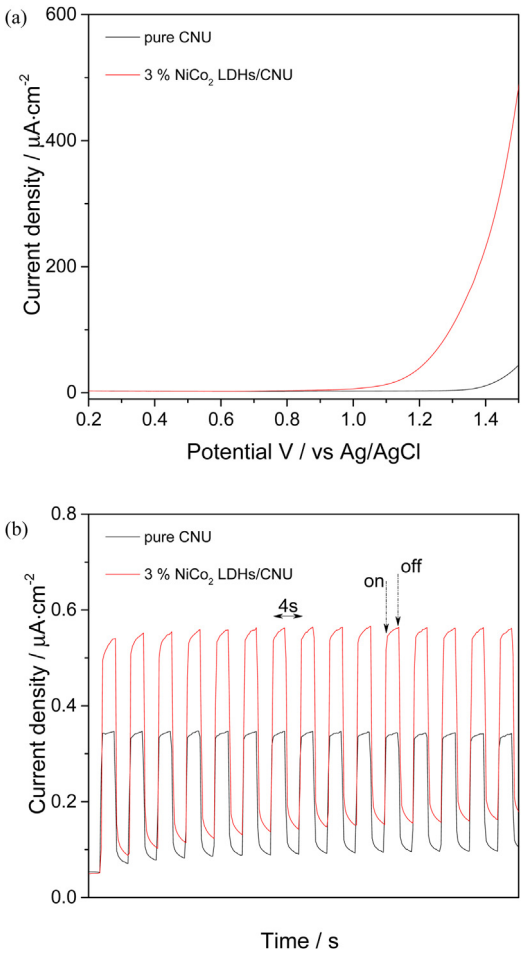

Fig. 6. (a) Polarization curves in dark and (b) transient photocurrent under visible light irradiation for the CNU and 3 wt.% $NiCo_2$ LDHs/CNU sample in a 0.2 M Na_2SO_4 aqueous solution (pH = 6.8).

tion. As shown in Fig. 7a, only trace amount of O_2 was generated when $NiCo_2$ LDHs was supported on light inert mesoporous SiO_2 (SBA-15) insulator under UV–vis light irradiation, implying that $NiCo_2$ LDHs alone is not active for photocatalytic O_2 evolution in semiconductor-free system. Besides, pure CNU without cocatalysts modification also showed low performance for water oxidation reaction (4.1 μmol·h^{-1}) even with UV–vis light irradiation, indicating that pure CNU was hindered by the huge energy barrier, being lack of surface active sites for oxygen evolution. It is excited to find that the as-prepared Ni_xCo_{3-x} LDHs/CNU samples showed much higher activities than the pure CNU, CoO_x/CNU and Co_3O_4/CNU samples, indicating the excellent performance of Ni-Co cocatalysts in promoting the water oxidation reaction. It should be noted that the activities could be optimized when adjusting the molecular ratio of Ni and Co in the Ni-Co cocatalysts. The optimum activity was achieved when Ni and Co molecular ratio is determined as 1:2. The O_2 evolution rate was determined as 26.7 μmol·h^{-1}, which is 6.5 times higher than that of the pure CNU, indicating the excellent role of the Ni-Co cocatalysts in promoting the water oxidation reaction. Besides, accompanied with the oxygen evolution, it could also be observed the nitrogen evolution. Because the valence holes presented low selectivity toward the oxidation reaction, they could also oxidize the CNU simultaneously to release nitrogen gas [12,19]. Note that the selectivity of light-induced holes toward water oxidation for O_2 evolution could be increased from 52% to 91% when $NiCo_2$ LDHs were used as the water oxidation cocatalysts. In the presence of LDHs, the photo-generated holes would fast transfer from CNU to the surface of LDHs, and subsequently participated in the surface water oxidation reaction without recombination. In this case, most of the holes would be utilized for water oxidation rather than self-oxidization of CNU (N^{3-} to N_2).

In addition, the water oxidation activities could be further optimized by adjusting the loading amount of $NiCo_2$ LDHs on the surface of the carbon nitride photocatalysts. As shown in Fig. 7b, the oxygen evolution rate fast increases when the loading contents were increased from 0 to 3 wt.%, which is mainly ascribed from the increased active sites. However, further increase in the contents of $NiCo_2$ LDHs would result in an evident decrease in the water oxidation activity. This is mainly because more loading contents of $NiCo_2$ LDHs would shield the light absorption efficiency of CNU, which no matter decrease the photocatalytic activities. Moreover, this $NiCo_2$ LDHs modified CNU polymers also showed robust stability towards solution corrosion. The total amounts of the evolved O_2 gases reached 89.4 μmol after 8 h of persistent reactions (Fig. 8a). The corresponding catalytic turnover number (TON) with respect to $NiCo_2$ LDHs is 5.6. However, the O_2 evolution rate was slightly decreased as the reaction time prolonged, which is mainly hindered by the in-situ deposition of Ag nanoparticles on the surface of CNU to decrease the light absorption efficiency. Notably, this $NiCo_2$ LDHs modified CNU polymer could also generate a considerable O_2 evolution activity of 5 μmol·h^{-1} even with visible light illumination (> 420 nm) (Fig. 8b), whereas pure CNU only produce negligible O_2

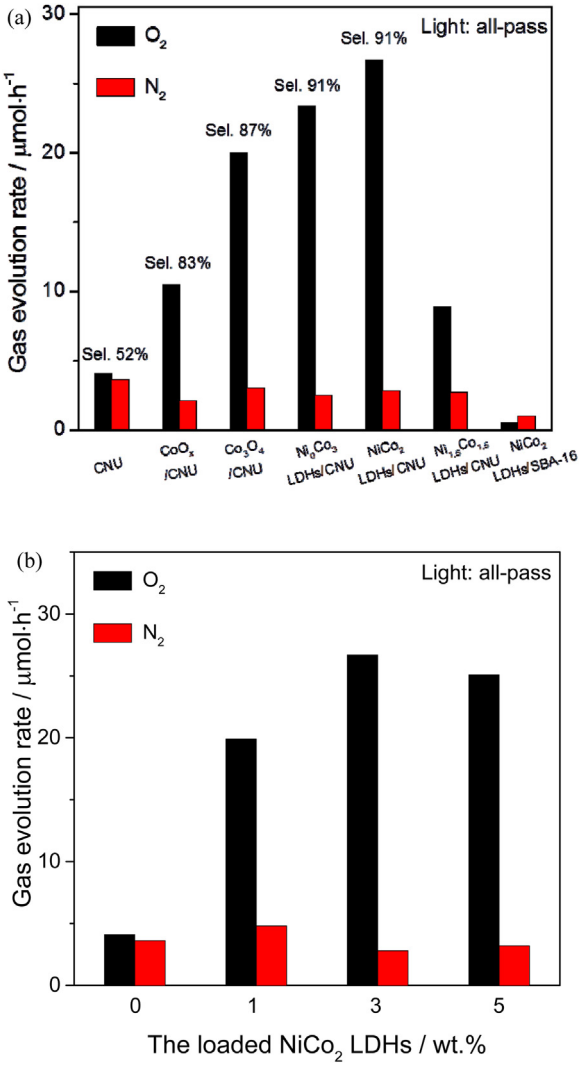

Fig. 7. (a) O_2 evolution rate for different co-catalyst-modified CNU samples under UV–vis light irradiation (λ > 300 nm); (b) O_2 evolution rate of CNU modified with different amount of $NiCo_2$ LDHs under UV–vis irradiation.

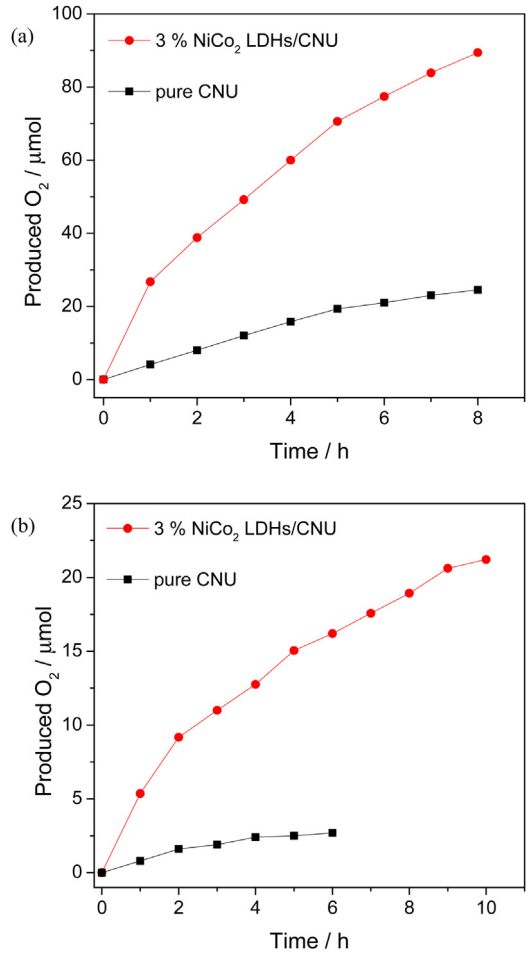

Fig. 8. Time course O_2 evolution for pure and 3 wt.% $NiCo_2$ LDHs modified CNU under (a) UV–vis light (λ > 300 nm) irradiation and (b) visible light irradiation (λ > 420 nm).

($0.8\ \mu mol \cdot h^{-1}$), once again underlining the huge advantage of the $NiCo_2$ LDHs in promoting the water oxidation reaction.

4. Conclusion

In conclusion, an efficient and sustainable water oxidation system has been fabricated when CNU and $NiCo_2$ LDHs were supported as light transducers and water oxidation cocatalysts, respectively. The interface charge carrier transfer could be largely accelerated and the water oxidation energy barrier was greatly decreased owing to the synergistic effect between $NiCo_2$ LDHs and CNU. The as-prepared $NiCo_2$ LDHs/CNU nanocomposites showed evidently enhanced water oxidation activity and selectivity under both UV and visible light irradiation in comparison with the inert pristine CNU. This study not only opens up a new strategy for the fabrication of sustainable water oxidation system comprising earth abundant elements to utilize solar energy in an efficient and economic manner, but also a conceptual development to rationally construct an effective interfacial 2D junctions between water oxidation catalysts and semiconductors. It will favor the development of energy based scaffold such as water splitting and CO_2 fixation.

Acknowledgement

This work is financially supported by the National Basic Research Program of China (2013CB632405), the National Natural Science Foundation of China (21425309 and 21761132002), and the 111 Project.

References

[1] F. Wen, C. Li, Acc. Chem. Res. 46 (2013) 2355–2364.
[2] Z. Zhang, J.T. Yates, Chem. Rev. 112 (2012) 5520–5551.
[3] K. Maeda, J. Photochem. Photobiol. C-Photochem. Rev. 12 (2011) 237–268.
[4] K. Maeda, K. Domen, Angew. Chem. Int. Ed. 51 (2012) 9865–9869.
[5] Y. Qu, X. Duan, Chem. Soc. Rev. 42 (2013) 2568–2580.
[6] M.-R. Gao, Y.-F. Xu, J. Jiang, Y.-R. Zheng, S.-H. Yu, J. Am. Chem. Soc. 134 (2012) 2930–2933.
[7] K. Maeda, K. Domen, J. Phys. Chem. Lett. 1 (2010) 2655–2661.
[8] M. Zhang, Z. Luo, M. Zhou, C. Huang, X. Wang, Sci. China Mater. 58 (2015) 867–876.
[9] J. Yang, D. Wang, H. Han, C. Li, Acc. Chem. Res. 46 (2013) 1900–1909.
[10] J. Ran, J. Zhang, J. Yu, M. Jaroniec, S.Z. Qiao, Chem. Soc. Rev. 43 (2014) 7787–7812.
[11] S. Chen, S. Shen, G. Liu, Y. Qi, F. Zhang, C. Li, Angew. Chem. Int. Ed. 54 (2015) 3047–3051.
[12] X. Wang, K. Maeda, A. Thomas, K. Takanabe, G. Xin, J.M. Carlsson, K. Domen, M. Antonietti, Nat. Mater. 8 (2009) 76–80.
[13] W.-J. Ong, L.-L. Tan, Y.H. Ng, S.-T. Yong, S.-P. Chai, Chem. Rev. 116 (2016) 7159–7329.
[14] X. Wang, S. Blechert, M. Antonietti, ACS Catal. 2 (2012) 1596–1606.
[15] Y. Zheng, L. Lin, B. Wang, X. Wang, Angew. Chem. Int. Ed. 54 (2015) 12868–12884.
[16] Z. Pan, Y. Zheng, F. Guo, P. Niu, X. Wang, ChemSusChem 10 (2017) 87–90.
[17] G. Zhang, Z.-A. Lan, L. Lin, S. Lin, X. Wang, Chem. Sci. 7 (2016) 3062–3066.
[18] D. Zheng, X.-N. Cao, X. Wang, Angew. Chem. Int. Ed. 55 (2016) 11512–11516.

[19] J. Zhang, M. Grzelczak, Y. Hou, K. Maeda, K. Domen, X. Fu, M. Antonietti, X. Wang, Chem. Sci. 3 (2012) 443–446.
[20] G. Zhang, C. Huang, X. Wang, Small 11 (2015) 1215–1221.
[21] G. Zhang, S. Zang, X. Wang, ACS Catal. 5 (2015) 941–947.
[22] G. Zhang, S. Zang, L. Lin, Z.-A. Lan, G. Li, X. Wang, ACS Appl. Mater. Inter. 8 (2016) 2287–2296.
[23] G. Zhang, S. Zang, Z.-A. Lan, C. Huang, G. Li, X. Wang, J. Mater. Chem. A 3 (2015) 17946–17950.
[24] M. Gong, Y. Li, H. Wang, Y. Liang, J.Z. Wu, J. Zhou, J. Wang, T. Regier, F. Wei, H. Dai, J. Am. Chem. Soc. 135 (2013) 8452–8455.
[25] V. Gupta, S. Gupta, N. Miura, J. Pow. Sour. 175 (2008) 680–685.
[26] J. Hong, W. Zhang, Y. Wang, T. Zhou, R. Xu, ChemCatChem 6 (2014) 2315–2321.
[27] J.H. Lee, J. Chang, J.-H. Cha, D.-Y. Jung, S.S. Kim, J.M. Kim, J. Chem. Eur. 16 (2010) 8296–8299.
[28] M.-Q. Zhao, Q. Zhang, J.-Q. Huang, F. Wei, Adv. Funct. Mater. 22 (2012) 675–694.
[29] G. Zhang, J. Zhang, M. Zhang, X. Wang, J. Mater. Chem. 22 (2012) 8083–8091.
[30] M. Zhang, X. Wang, Energy Environ. Sci. 7 (2014) 1902–1906.
[31] Z. Lin, X. Wang, Angew. Chem. Int. Ed. 52 (2013) 1735–1738.
[32] Z. Zhao, H. Wu, H. He, X. Xu, Y. Jin, Adv. Funct. Mater. 24 (2014) 4698–4705.
[33] C. Yuan, J. Li, L. Hou, X. Zhang, L. Shen, X.W. Lou, Adv. Funct. Mater. 22 (2012) 4592–4597.
[34] B. Cui, H. Lin, Y.-Z. Liu, J.-B. Li, P. Sun, X.-C. Zhao, C.-J. Liu, J. Phys. Chem. C 113 (2009) 14083–14087.
[35] M.C. Biesinger, B.P. Payne, A.P. Grosvenor, L.W.M. Lau, A.R. Gerson, R.S.C. Smart, Appl. Surf. Sci. 257 (2011) 2717–2730.
[36] Y. Zhang, J. Liu, G. Wu, W. Chen, Nanoscale 4 (2012) 5300–5303.